

Published in final edited form as:

J Immunol Methods. 2005 July ; 302(1-2): 90–98. doi:10.1016/j.jim.2005.04.018.

Laser capture microdissection and single-cell RT-PCR without RNA purification

Kathryne Melissa Keays^a, Gregory P. Owens^a, Alanna M. Ritchie^a, Donald H. Gilden^{a,b}, and Mark P. Burgoon^{a,*}

^aDepartment of Neurology, University of Colorado Health Sciences Center, 4200 East 9th Avenue, Mail Stop B182, Denver, CO 80262, United States

^bDepartment of Microbiology, University of Colorado Health Sciences Center, Denver, CO, United States

Abstract

Chronic infectious diseases of the central nervous system (CNS) are characterized by intrathecal synthesis of increased amounts of immunoglobulin G (IgG) directed against the agent that causes disease. In other inflammatory CNS diseases such as multiple sclerosis and CNS sarcoid, the targets of the humoral immune response are uncertain. To identify the IgGs expressed by individual CD38⁺ plasma cells seen in human brain sections, we merged the techniques of laser capture microdissection (LCM) and single-cell RT-PCR. Frozen brain sections from a patient who died of subacute sclerosing panencephalitis (SSPE), were rapidly immunostained and examined by LCM to dissect individual CD38⁺ cells. After cell lysis, we developed two techniques for reverse-transcription (RT) of unpurified total RNA in the cell lysates. The first method performed repeated and rapid freeze–thawing, followed by centrifugation of the cell lysate into tubes for subsequent RT. The second, more successful method performed RT in situ on detergent-solubilized cells directly on the cap surface; subsequent nested PCR identified heavy and light chain sequences expressed by two-thirds of individually isolated plasma cells. These techniques will streamline the identification of gene expression products in single cells from complex tissues and have the potential to identify IgGs expressed in the CNS of inflammatory diseases of unknown etiology.

Keywords

Laser capture microdissection; Single cell RT-PCR; Plasma cells; Subacute sclerosing panencephalitis; IgG

1. Introduction

The development of LCM has enabled genetic analysis of groups of similar cells in cancers (Emmert-Buck et al., 1996; Bonner et al., 1997; Glasow et al., 1998; Specht et al., 2002) and has allowed microarray comparisons in multiple tissues (Luo et al., 1999; Fuller et al., 2003; Upson et al., 2004; Player et al., 2004). Additional techniques have extended the potential of LCM. For example, immunohistochemical staining before LCM identified targeted cell types when morphological criteria failed (Fend et al., 1999; Ball et al., 2002; Vincent et al., 2002). The study of smaller numbers of cells often required preamplification of RNA from LCM-captured cells (Goldsworthy et al., 1999; Bonaventure et al., 2002; Mikulowska-

Mennis et al., 2002; Ginsberg and Che, 2004) and rapid staining to preserve nucleic acid integrity in order to generate accurate gene expression profiles (Fend et al., 1999; Mojsilovic-Petrovic et al., 2004).

Extension of LCM from small populations of cells to individual cells has relied on PCR amplification of cell DNA (Suarez-Quian et al., 1999; Obiakor et al., 2002; Orba et al., 2003) or the perceived need to purify the very small amount of RNA, approximately 20 pg from a single captured cell for RT and PCR (Jin et al., 2001; Parlato et al., 2002; Michel et al., 2003; Kamme et al., 2004; Lu et al., 2004; Fassunke et al., 2004). Hydraulic microdissection has also been coupled with nested-PCR amplification of genomic DNA to identify sequences in single B cells (Obiakor et al., 2002). To analyze the IgG expressed by individual plasma cells resident in the brains of patients with inflammatory CNS disease, without any delay that might degrade RNA, we optimized rapid protocols to immunostain and microdissect individual CD38⁺ plasma cells in sections of archived frozen brain from a patient who died of SSPE, a progressive fatal encephalitis caused by measles virus. Herein, we describe two methods to use RT-PCR on lysates of individual plasma cells that enables PCR amplification and analysis of expressed heavy and light chain IgG sequences.

2. Materials and methods

2.1. Tissue processing and immunohistochemistry

Archival SSPE brain was frozen 6 h after death and stored at -70°C . Brain was embedded in OCT (Sakura Finetek U.S.A., Inc., Torrance, CA) on liquid nitrogen and equilibrated to -30°C overnight. Cryostat blades, tools, surfaces, slides and staining vessels were pretreated with RNase Zap (Ambion, Austin TX), and all solutions were prepared with DEPC-treated water containing 200 units/ml RNase inhibitor (Fisher Scientific, Pittsburgh, PA). Sections ($7\ \mu\text{m}$) were cut at -30°C and immediately placed onto uncharged “non-plus” slides (Fisher). After acetone fixation for 5 min at -20°C and treatment with 0.1% hydrogen peroxide for 30 s, slides were rapidly immunostained for CD38⁺ cells on a pre-chilled steel block maintained at 0°C . Sections were blocked in 10% goat serum in PBS for 2 min, followed by incubation for 10 min with a 1:50 dilution of mouse anti-human CD38 (Dako Cytomation, Carpinteria, CA) in 5% goat serum in PBS. After rinsing in PBS, sections were incubated for 5 min with a 1:100 dilution of HRP-labeled horse-anti-mouse antibody (Vector Labs, Burlingame, CA) in 5% goat serum in PBS. Sections were rinsed in PBS and incubated for 5 min with DAB substrate (Dako), counterstained with filtered hematoxylin (Sigma, St. Louis, MO) for 40 s, dehydrated in a series of nuclease-free graded alcohols (HistoGene Kit, Arcturus) (75% for 30 s, 95% for 30 s, 100% for 3 min), and cleared in two changes of xylenes for 2 min each. To maximize RNA preservation, tissue exposure to aqueous solutions was limited to less than 25 min.

2.2. Laser capture microdissection

LCM was performed on a PixCell Iie microscope (Arcturus Engineering, Mountain View, CA) with CapSure HS caps (Arcturus) using a pulse power of 70 mW, a $7.5\text{-}\mu\text{m}$ laser spot diameter, pulse duration of 5 ms and a target voltage of 170 mV. Tissue heterogeneity/cell targeting was visualized by applying xylene ($10\ \mu\text{l}$) to sections. When the cell of interest was identified and xylene had evaporated, the cell was captured. Frequently, cells adjacent to the laser-targeted cell were co-isolated onto the cap; they were removed by pressing the cap surface onto a sterile adhesive-backed paper (Post-it note, 3M, St. Paul, MN). Extraction reservoirs were placed on the caps, and the assemblies were immediately placed in a tray (Arcturus) at -20°C until completion of LCM.

2.3. RT-PCR

Six conditions using three CD38+ cells per cap were tested to determine optimal protocols for RT. In five of the conditions, cells were lysed and centrifuged into tubes for RT, whereas in the sixth method, RT was performed on the lysate directly on the cap surface. All of the lysis conditions were performed in 21 μ l 1 \times SuperScript III first-strand RT buffer (Invitrogen, Carlsbad, CA) containing 1% or 3% NP40, which was added to the extraction reservoirs on all caps. The first five lysis conditions were carried out by three freeze–thaw cycles over 20 min with 1% NP40 on dry ice as described (To et al., 1998), or with 1% NP40 at 80 $^{\circ}$ C, or with 3% NP40 at 42 $^{\circ}$ C, or with 1% NP40 at 42 $^{\circ}$ C, or with 3% NP40 at 80 $^{\circ}$ C (one cap with three cells, one cap with 10 cells) for 20 min. 500- μ l GeneAmp tubes (Perkin-Elmer, Wellesley, MA) were fitted onto the reservoirs, and the inverted assembly was microcentrifuged at 6000 rpm to collect the lysis products from all caps. The sixth lysis condition was carried out with 21 μ l 1 \times SuperScript III first-strand RT buffer containing 1% NP40 at 42 $^{\circ}$ C for 20 min, after which the RT reaction was performed on the cap surface. Twelve to 14 individual plasma cells were captured in each LCM session. Positive and negative control tubes in each RT experiment used 10 pg of total RNA purified from the IgG-expressing human lymphoblastoid B cell line ARH-77 (ATCC #CRL-1621), with and without RT enzyme, respectively.

RT was performed as described (Owens et al., 2003). Briefly, 2 μ l 5 \times first strand buffer, 0.5 μ l random hexamers (Invitrogen), 0.5 μ l of an anti-sense IgG1 constant domain primer (CH5A), 1 μ l H₂O and 0.5 μ l RNase inhibitor (Fisher) were added to each tube or the cap. The tubes, or the cap, were incubated at 65 $^{\circ}$ C for 3 min, and then at 25 $^{\circ}$ C for 3 min. To each reaction, 3 μ l 0.1 M dTT, 1.5 μ l dNTPs, 0.5 μ l RNase inhibitor, and 0.5 μ l SuperScript III (Invitrogen) were added, followed by incubation at 37 $^{\circ}$ C for 60 min, and at 70 $^{\circ}$ C for 10 min. The product of the RT reaction performed on the cap was centrifuged into a tube, and 5- μ l aliquots from all reactions were subjected to nested PCR amplification of IgG heavy or light chain sequences as described (Owens et al., 2003). We then compared the freeze–thaw method with performance of RT on the cap surface, using six LCM caps per method and one or three cells per cap. PCR products were resolved on 2% agarose gels. Appropriately sized bands were excised and DNA was purified using the MinElute Gel Extraction kit (Qiagen, Valencia, CA). The IgG amplification products were confirmed by sequencing at the University of Colorado Health Sciences Cancer Center DNA Analysis and Sequencing Core (Denver, CO), and analyzed in DNAsis Max (Miraibio Inc, Alameda, CA). After each experiment, all caps were stored at -80° C. Caps were thawed and RT was repeated directly on the cap surface. Nested PCR amplification of the cDNA was also performed for kappa and lambda light chains as described (Owens et al., 2003).

3. Results

All steps were optimized to enhance LCM and RT-PCR of single immunostained cells. Several features of slide preparation before immunostaining were critical. First, frozen SSPE brain sections were prepared under RNase-free conditions. Besides the normal precautions of wearing gloves at all times and using RNase-free (DEPC-treated) H₂O in all solutions, the cryostat blade, microscope slides and staining vessels were all routinely treated with the RNase inhibitor RNase Zap after two early attempts failed to obtain RT-PCR amplifiable material from sections cut on new slides with a new blade. Second, slides sectioned before fixation were maintained at temperatures below -20° C to ensure minimal adhesion of the section to the slide for successful LCM; three sessions at the LCM microscope in which sectioned slides were briefly thawed before fixation at -20° C did not successfully remove cells from the section. Third, the use of non-plus slides was important for microdissection of cells from the section; repeated attempts to microdissect from immunostained brain sections on charged (+) slides resulted in lifting of only 10–20% of targeted cells from the slide.

Freshly cut sections were acetone-fixed at -20°C , briefly treated with 0.1% hydrogen peroxide and immunostained. Mouse anti-CD38 antibody identified plasma cells, which were well-separated (Fig. 1a). To ensure RNA integrity, exposure to aqueous solutions during staining was limited to 25 min, and RNase inhibitor was added to every buffer. Peroxidase-conjugated horse-anti-mouse IgG antibody and DAB were used to visualize the stained cells. Two early attempts to use alkaline-phosphatase-conjugated anti-mouse IgG and New Fuschin substrate were unsuccessful when the New Fuschin disappeared after xylene treatment. Use of DAB provided permanent staining. Pretreatment of the slides with hydrogen peroxide dramatically reduced background staining but was limited to 30 s, since in two earlier experiments, higher concentrations or longer incubations with hydrogen peroxide damaged tissue morphology. After hematoxylin counterstaining, sections were dehydrated with graded alcohols and xylene before LCM. Complete dehydration of the sections was achieved by including molecular sieves in the 100% ethanol used in the final ethanol incubation, for which the HistoGene kit (Arcturus) is ideally designed. Complete dehydration was important to the dissection of cells during LCM and was improved by extending the 100% ethanol stage to 3 min. Slides could be maintained in xylene for several days before successful LCM, but RNA integrity was compromised by the prolonged slide storage (data not shown).

LCM was used to microdissect individual CD38+ plasma cells onto separate caps (Fig. 1). A droplet of xylene was first added to the dehydrated brain section to restore color balance and visualize the stained cells. However, complete evaporation of the xylene was necessary before positioning the extraction cap over the targeted cell so the laser-pulsed cells could adhere to the cap (Fig. 1b). When surrounding cells were co-dissected with the targeted cell, the cap surface was gently pressed onto an adhesive-backed paper to remove adjacent cells. Extraction reservoirs were added to the caps and the assemblies were stored at -20°C until 12 cells were individually obtained onto caps. The $7.5\ \mu\text{m}$ laser spot size was optimal for lifting the fewest cells from brain sections. In general, a lower pulse duration and higher power setting enabled a more precise capture.

After the targeted cells were transferred to the caps, standard methods for RNA extraction and purification would have been both labor-intensive and costly, involving additional incubation times and treatments of more than 100 caps with extraction buffers before RT. We therefore compared various methods for rapid and efficient RT, with the aims of performing RT-PCR using the unfractionated cell lysate and of testing methods to remove the lysate from caps before RT or to enable RT directly on the cap surface without prior extraction. Six strategies were tested: lysis by three freeze-thaw cycles (To et al., 1998); lysis at 80°C ; 1% or 3% NP40; 3% NP40 and lysis at 80°C (from one cap with three cells, and from one cap with 10 cells); and performing RT on the cap surface after 1% NP40 treatment. Two of these strategies, i.e., lysis by rapid freeze-thaw cycles followed by centrifugation into a reaction tube, and conducting RT on the cap surface after incubation with 1% NP40 at 42°C , yielded products after nested PCR of IgG heavy chain variable regions (Fig. 2). RT controls were always performed in parallel tubes with 10 pg of total RNA purified from the IgG-expressing ARH-77 lymphoma cells.

Next, we directly compared the two successful methods: freeze-thawing to remove the cell lysate from the cap before performing RT; and performing RT on the lysate in situ, directly on the cap surface. Each method was tested on four caps containing one immunostained CD38+ cell per cap, and on two caps containing three stained cells per cap. The caps for both methods were collected randomly to ensure that the storage time of each cap did not influence the success of RT performed after all 12 caps had been obtained. Four of six samples processed on the cap successfully amplified HC products, while one of six samples from the freeze-thaw cycles yielded only barely detectable products; the remaining caps

were negative (Fig. 3). Three cells per cap did not increase the amount of PCR amplification product over that observed with one cell. Finally, the twelve caps used for this comparative analysis were frozen, and RT was repeated on all cap surfaces the next day (Fig. 4). This produced additional PCR products from caps that were originally positive, including an intense PCR product from the freeze–thaw cap that was originally only weakly positive, and two positive PCR products from caps that were previously negative. In subsequent experiments, repeated RT on refrozen caps routinely revealed several more positives than were originally identified (data not shown).

These tests resulted in a protocol that was repeated on more than 100 caps, in which RT was performed on individual CD38+ cells on the cap surface, before centrifuging the RT products into a tube. Judged by successful PCR-amplification of IgG heavy chains and light chains, SuperScript III reverse transcriptase routinely synthesized cDNA from two-thirds of approximately 120 cap surfaces containing single CD38+ plasma cells. A typical experiment from one LCM session showed that after RT was performed on the surface of 13 caps, nested PCR of heavy chain IgG sequences yielded ten positive products (Fig. 5a). Those ten RT products that yielded heavy chain sequences were also subjected to nested PCR for kappa light chain sequences, and amplified seven appropriately sized PCR products (Fig. 5b). Early experiments to detect actin PCR products after these protocols did not detect larger numbers of successful amplification products, suggesting that the negatives we encountered were not simply IgG-negative cells. When the SuperScript III enzyme was omitted from caps or from 11 negative control reactions with B lymphoma cell RNA, amplified IgG sequences were never observed by nested PCR (data not shown).

4. Discussion

We have described protocols optimized to: 1) rapidly immunostain archival brain sections and identify individual (CD38+) plasma cells; 2) capture individual CD38+ cells by LCM; and 3) perform single-cell RT-PCR on the expressed Ig transcripts for sequence analysis. The most successful strategy microdissected single immunostained CD38+ plasma cells from frozen brain sections by LCM, and after lysis, allowed RT in situ on the cap surface without RNA purification. Using this strategy, more than 100 individual CD38+ cells were rapidly isolated from sections of an SSPE brain and analyzed for individually expressed IgG antibodies (Burgoon et al., PNAS, in press). Immunostaining protocols before LCM must be conducted quickly to preserve RNA (Fend et al., 1999; Burgess and McParland, 2002; Mojsilovic-Petrovic et al., 2004). However, since LCM was first described, few studies have examined RNA expression in individual cells from human post-mortem CNS (Bahn et al., 2001; Lu et al., 2004), likely reflecting the challenge of isolating single cells from a complex tissue and the subsequent purification of 10–20 pg of total RNA from each cell for analysis (Michel et al., 2003; Parlato et al., 2002). One advantage of our study is the need to isolate only small clusters of 5–10 cells to analyze single immunostained cells contained therein, since the plasma cell is the only one that expresses IgG. Several caps contained multiple amplified IgG sequences, which may have resulted from the simultaneous expression of two IgG sequences by a single cell as may occur with receptor editing (Kouskoff and Nemazee, 2001), or from expression of a nearby CD38-negative B cell that was accidentally captured with the CD38+ plasma cell. Double-staining protocols for CD38+ plasma cells and CD19+ B cells might reduce the frequency of capturing multiple IgG-expressing cells.

Previous studies have determined that the duration of the LCM process may adversely affect RNA integrity (Michel et al., 2003; Nawshad et al., 2004), and that mRNA quality is better in frozen sections than paraffin-embedded tissues (Fend and Raffeld, 2000). Our methods described herein streamline the process to analyze RNA contained in archived frozen brain tissue without purification or further risk of degradation. Features of specific tissues, such as

low pH or high concentrations of degradative enzymes, may influence RNA stability throughout the staining or LCM procedures (Kingsbury et al., 1995; Harrison et al., 1995; Bahn et al., 2001). Tissue treatment with 30% sucrose has also been suggested to preserve morphology and RNA integrity (Parlato et al., 2002). The agonal status (particularly hypoxia in prolonged agonal states) and storage temperature of tissue are also important (Bahn et al., 2001), and might be further inducement for speed and cold temperatures. Cresyl violet, thionin, hematoxylin and eosin, but not silver stain or acridine orange, have been recommended for use in immunostaining (Ginsberg et al., 2004). Other influences on the success of RT-PCR suggest the desirability of precipitative fixatives such as ethanol and acetone rather than cross-linking fixatives such as formalin (Goldsworthy et al., 1999). We have incorporated many of these earlier findings into studies of the IgG repertoire expressed by single plasma cells in frozen, archived SSPE brain tissue.

Earlier reports have suggested that staining times in aqueous media should be limited to less than 20 min (Fend et al., 1999; Mojsilovic-Petrovic et al., 2004). The staining protocol used here is completed in less than 25 min and the total time required from tissue sectioning until cDNA production is less than 4 h. Careful RNase-free conditions throughout the entire procedure, conducting immunostaining on ice, and the inclusion of RNase inhibitor at every step are logical precautions to preserve RNA. Allowing slides to thaw during sectioning also prevented the dissection of cells, possibly due to the activation of endogenous glycolases, which form a strong bond with glass when hydrated. Sections prepared for LCM were maintained at -30°C until fixation in -20°C acetone. Essential to capturing cells from tissue sections was complete dehydration after immunostaining, in agreement with earlier studies (Fend et al., 1999; Ball et al., 2002). The use of non-plus slides was helpful since frozen tissue adhered too strongly to charged slides for effective laser dissection. This application must be carefully balanced against the possibility of picking up additional cells with the targeted cell when tissue adheres loosely to the slide. An effective method to remove extraneous material after LCM was to gently press the cap surface against a sterile, adhesive-backed paper such as a “Post-It note” (3M). Alternatively, prep strips provided by Arcturus may be applied to the cap. Only the cell area directly below the laser pulse remained visibly attached to the thermoplastic coating on the cap surface after application of the paper (data not shown).

LCM was most effective when tissue was sectioned on the same day as cell capture (LCM on sections prepared the previous day lifted cells, but RT-PCR was unsuccessful) (data not shown). After cell capture by LCM, RNA purification or extraction was not desirable due to: (1) the limited amount of RNA contained on each cap; (2) the number of samples to be individually treated and analyzed; (3) the time required to treat the greater number of single-cell samples; and (4) the cost involved in hundreds of RNA purifications needed for a repertoire of individual cells. Furthermore, extraction and purification protocols, both customized and those outlined in commercial kits, are intended for much larger amounts of RNA. Therefore, we sought to perform RT-PCR directly on cell lysate on the cap surfaces, without prior RNA purification. Although this method was superior to freeze–thawing under the conditions analyzed, repeating RT on refrozen caps may be useful to obtain additional PCR products on caps that were previously negative and may even supplement cDNA recovered from the positive caps. This accelerated method probably prevented RNA degradation or loss that occurs during purification steps. Although RNase-free DNase may be added to the cell lysis step to ensure amplification only from reverse-transcribed cDNA, we did not treat samples in this study because genomic DNA could not contribute to our nested RT-PCR analysis of IgG sequences. The PCR primers that we used would have amplified a different-sized product from the recombined genomic DNA in the plasma cells than from the transcripts (Abbas and Lichtman, 2003). Furthermore, surrounding cells that were co-isolated but were not in the B cell lineage would not contain a recombined IgG

variable region in their genomes. Finally, when RT was not added to control caps, PCR products were never observed.

Overall, we have described techniques that allow genetic analysis of single plasma cells in the complex milieu of the brain. Although it remains difficult to isolate a single cell by LCM reliably, such analysis is possible in well-defined circumstances after immunostaining single, well-separated cells surrounded by unstained tissue. The presented features critical to staining, LCM and RT procedures allowed successful identification of IgG expression in a repertoire of plasma cells in an efficient and cost-effective manner. These IgG sequences can then be functionally characterized after cloning into suitable expression vectors to generate recombinant immunoglobulins (Burgoon et al., PNAS, in press). These techniques will permit the application of LCM to gene expression analysis in single cells without the need for RNA purification.

Abbreviations

CNS	central nervous system
IgG	immunoglobulin G
LCM	laser capture microdissection
RT	reverse transcription
SSPE	subacute sclerosing panencephalitis
PCR	polymerase chain reaction
DEPC	diethylpyrocarbonate
PBS	phosphate-buffered saline
HRP	horseradish peroxidase
DAB	diaminobenzidine
cDNA	complementary DNA

Acknowledgments

SSPE brain was kindly provided by the National Neurological Research Specimen Bank, Veterans Administration Medical Center (Los Angeles, CA). We thank Pradeep R. Rai, UCHSC, for providing advice during this work, Marina Hoffman for editorial review, and Cathy Allen for preparing the manuscript. This work was supported by grants from the National Institutes of Health NS41549 (to M.P.B.) and NS32623 (to D.H.G., M.P.B. and G.P.O.).

References

- Abbas, AK.; Lichtman, AH. Cellular and Molecular Immunology. 5th edition. Philadelphia, PA: Saunders; 2003.
- Bahn S, Augood S, Standaert DG, Starkey M, Emson PC. Gene expression profiling in the post-mortem human brain—no cause for dismay. *J. Chem. Neuroanat.* 2001; 22:79. [PubMed: 11470556]
- Ball HJ, McParland B, Driussi C, Hunt NH. Isolating vessels from the mouse brain for gene expression analysis using laser capture microdissection. *Brain Res. Protoc.* 2002; 9:206.
- Bonaventure P, Guo HQ, Tian B, Liu XJ, Bittner A, Roland B, Salunga R, Ma XJ, Kamme F, Meurers B, Bakker M, Jurzak M, Leysen JE, Erlander MG. Nuclei and subnuclei gene expression profiling in mammalian brain. *Brain Res.* 2002; 943:38. [PubMed: 12088837]
- Bonner RF, Emmert-Buck M, Cole K, Pohida T, Chuaqui R, Goldstein S, Liotta LA. Cell sampling—Laser capture microdissection: molecular analysis of tissue. *Science.* 1997; 278:1481. [PubMed: 9411767]

- Burgess JK, McParland BE. Analysis of gene expression. *Methods Enzymol.* 2002; 356:259. [PubMed: 12418204]
- Burgoon MP, Keays KM, Owens GP, Ritchie AM, Rai PR, Cool CD, Gilden DH. Laser-capture microdissection of plasma cells from subacute sclerosing panencephalitis brain reveals intrathecal disease-relevant antibodies. *Proc. Natl. Acad. Sci.* 2005 in press.
- Emmert-Buck MR, Bonner RF, Smith PD, Chuaqui RF, Zhuang Z, Goldstein SR, Weiss RA, Liotta LA. Laser capture microdissection. *Science.* 1996; 274:998. [PubMed: 8875945]
- Fassunke J, Majores M, Ullmann C, Elger CE, Schramm J, Wiestler OD, Becker AJ. In situ-RT and immunolaser microdissection for mRNA analysis of individual cells isolated from epilepsy-associated glioneuronal tumors. *Lab. Invest.* 2004; 84:1520. [PubMed: 15311215]
- Fend F, Raffeld M. Laser capture microdissection in pathology. *J. Clin. Pathol.* 2000; 53:666. [PubMed: 11041055]
- Fend F, Emmert-Buck MR, Chuaqui R, Cole K, Lee J, Liotta LA, Raffeld M. Immuno-LCM: laser capture microdissection of immunostained frozen sections for mRNA analysis. *Am. J. Pathol.* 1999; 154:61. [PubMed: 9916919]
- Fuller AP, Palmer-Toy D, Erlander MG, Sgroi DC. Laser capture microdissection and advanced molecular analysis of human breast cancer. *J. Mammary. Gland. Biol.* 2003; 8:335.
- Ginsberg SD, Che SL. Combined histochemical staining, RNA amplification, regional, and single cell cDNA analysis within the hippocampus. *Lab. Invest.* 2004; 84:952. [PubMed: 15107803]
- Glasow A, Haidan A, Gillespie J, Kelly PA, Chrousos GP, Bornstein SR. Differential expression of prolactin receptor (PRLR) in normal and tumorous adrenal tissues: separation of cellular endocrine compartments by laser capture microdissection (LCM). *Endocr. Res.* 1998; 24:857. [PubMed: 9888587]
- Goldsworthy SM, Stockton PS, Trempus CS, Foley JF, Maronpot RR. Effects of fixation on RNA extraction and amplification from laser capture microdissected tissue. *Mol. Carcinog.* 1999; 25:86. [PubMed: 10365909]
- Harrison SM, Dunwoodie SL, Arkell RM, Lehrach H, Beddington RS. Isolation of novel tissue-specific genes from cDNA libraries representing the individual tissue constituents of the gastrulating mouse embryo. *Development.* 1995; 121:2479. [PubMed: 7671812]
- Jin L, Tsumanuma I, Ruebel KH, Bayliss JM, Lloyd RV. Analysis of homogeneous populations of anterior pituitary folliculostellate cells by laser capture microdissection and reverse transcription-polymerase chain reaction. *Endocrinology.* 2001; 142:1703. [PubMed: 11316732]
- Kamme F, Zhu J, Luo L, Yu J, Tran DT, Meurers B, Bittner A, Westlund K, Carlton S, Wan J. Single-cell laser-capture microdissection and RNA amplification. *Methods Mol. Med.* 2004; 99:215. [PubMed: 15131340]
- Kingsbury AE, Foster OJ, Nisbet AP, Cairns N, Bray L, Eve DJ, Lees AJ, Marsden CD. Tissue pH as an indicator of mRNA preservation in human post-mortem brain. *Mol. Brain Res.* 1995; 28:311. [PubMed: 7723629]
- Kouskoff V, Nemazee D. Role of receptor editing and revision in shaping the B and T lymphocyte repertoire. *Life Sci.* 2001; 69:1105. [PubMed: 11508343]
- Lu LX, Neff F, Dun Z, Hemmer B, Oertel WH, Schlegel J, Hartmann A. Gene expression profiles derived from single cells in human postmortem brain. *Brain Res. Protoc.* 2004; 13:18.
- Luo L, Salunga RC, Guo HQ, Bittner A, Joy KC, Galindo JE, Xiao HN, Rogers KE, Wan JS, Jackson MR, Erlander MG. Gene expression profiles of laser-captured adjacent neuronal subtypes. *Nat. Med.* 1999; 5:117. [PubMed: 9883850]
- Michel C, Desdouets C, Sacre-Salem B, Gautier JC, Roberts R, Boitier E. Liver gene expression profiles of rats treated with clofibrac acid — comparison of whole liver and laser capture microdissected liver. *Am. J. Pathol.* 2003; 163:2191. [PubMed: 14633594]
- Mikulowska-Mennis A, Taylor TB, Vishnu P, Michie SA, Raja R, Horner N, Kunitake ST. High-quality RNA from cells isolated by laser capture microdissection. *BioTechniques.* 2002; 33:176. [PubMed: 12139243]
- Mojsilovic-Petrovic J, Nestic M, Pen A, Zhang WD, Stanimirovic D. Development of rapid staining protocols for laser-capture microdissection of brain vessels from human and rat coupled to gene expression analyses. *J. Neurosci. Methods.* 2004; 133:39. [PubMed: 14757343]

- Nawshad A, LaGamba D, Olsen BR, Hay ED. Laser capture microdissection (LCM) for analysis of gene expression in specific tissues during embryonic epithelial–mesenchymal transformation. *Dev. Dyn.* 2004; 230:529. [PubMed: 15188437]
- Obiakor H, Sehgal D, Dasso JF, Bonner RF, Malekafzali A, Mage RG. A comparison of hydraulic and laser capture microdissection methods for collection of single B cells, PCR and sequencing of antibody VDJ. *Anal. Biochem.* 2002; 306:55. [PubMed: 12069414]
- Orba Y, Tanaka S, Nishihara H, Kawamura N, Itoh T, Shimizu M, Sawa H, Nagashima K. Application of laser capture microdissection to cytologic specimens for the detection of immunoglobulin heavy chain gene rearrangement in patients with malignant lymphoma. *Cancer Cytopathol.* 2003; 99:198.
- Owens GP, Ritchie AM, Burgoon MP, Williamson RA, Corboy JR, Gilden DH. Single-cell repertoire analysis demonstrates that clonal expansion is a prominent feature of the B cell response in multiple sclerosis cerebrospinal fluid. *J. Immunol.* 2003; 171:2725. [PubMed: 12928426]
- Parlato R, Rosica A, Cuccurullo V, Mansi L, Macchia P, Owens JD, Mushinski JF, De Felice M, Bonner RF, Di Lauro R. A preservation method that allows recovery of intact RNA from tissues dissected by laser capture microdissection. *Anal. Biochem.* 2002; 300:139. [PubMed: 11779104]
- Player A, Barrett JC, Kawasaki ES. Laser capture microdissection, microarrays and the precise definition of a cancer cell. *Expert. Rev. Mol. Diagn.* 2004; 4:831. [PubMed: 15525225]
- Specht K, Kremer M, Muller U, Dirnhofer S, Rosemann M, Hoffler H, Quintanilla-Martinez L, Fend F. Identification of cyclin D1 mRNA overexpression in B-cell neoplasias by real-time reverse transcription-PCR of microdissected paraffin sections. *Clin. Cancer Res.* 2002; 8:2902. [PubMed: 12231535]
- Suarez-Quian CA, Goldstein SR, Pohida T, Smith PD, Peterson JI, Wellner E, Ghany M, Bonner RF. Laser capture microdissection of single cells from complex tissues. *BioTechniques.* 1999; 26:328. [PubMed: 10023545]
- To MD, Done SJ, Redston M, Andrulis IL. Analysis of mRNA from microdissected frozen tissue sections without RNA isolation. *Am. J. Pathol.* 1998; 153:47. [PubMed: 9665464]
- Upson JJ, Stoyanova R, Cooper HS, Patriotis C, Ross EA, Boman B, Clapper ML, Knudson AG, Bellacosa A. Optimized procedures for microarray analysis of histological specimens processed by laser capture microdissection. *J. Cell. Physiol.* 2004; 201:366. [PubMed: 15389559]
- Vincent VAM, Devoss JJ, Ryan HS, Murphy GM. Analysis of neuronal gene expression with laser capture micro-dissection. *J. Neurosci. Res.* 2002; 69:578. [PubMed: 12210823]

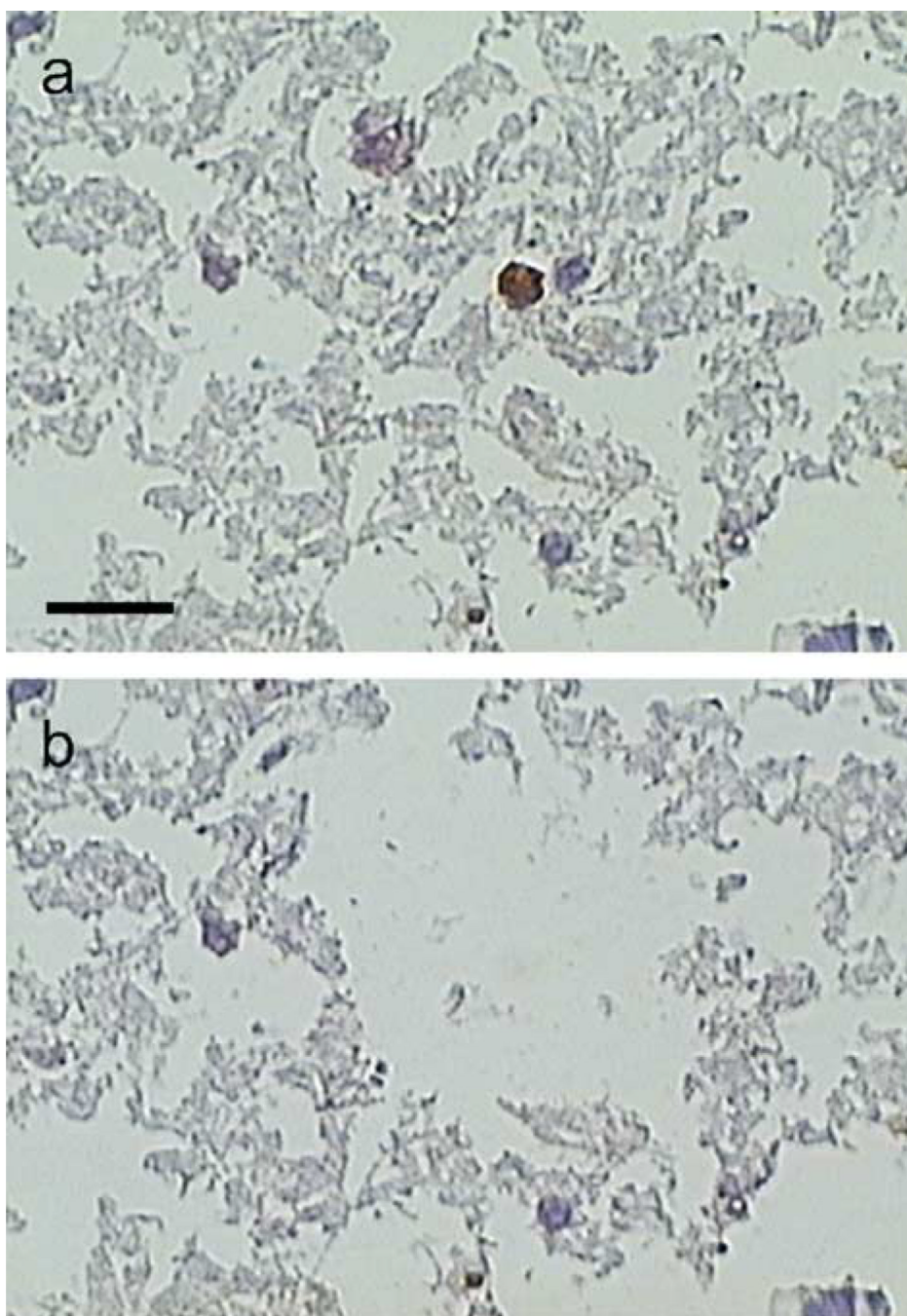


Fig. 1. Laser capture microdissection of CD38+ plasma cells. (a) A single plasma cell identified by DAB staining (brown) for CD38. (b) The stained cell and adjacent unstained cells were successfully removed by microdissection. Bar=20 μ m.

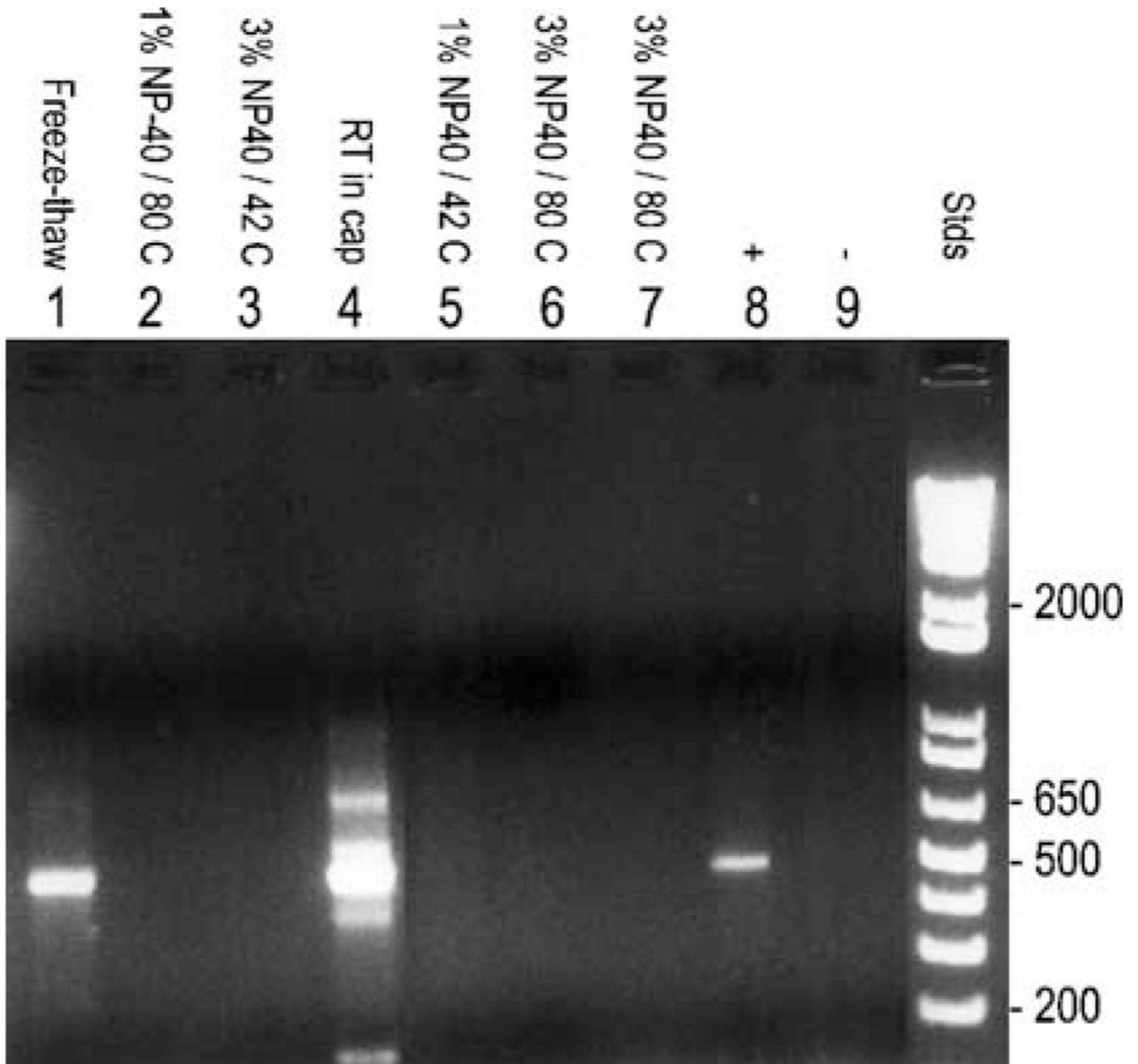


Fig. 2.

Nested PCR of heavy chain IgG after preparation of RNA for RT by different methods. Six conditions (see Materials and methods) were used before RT of total RNA from microdissected cells. Only the freeze-thaw method (lane 1) and RT performed on the cap surface (lane 4) yielded positive PCR products. Lane 8 shows an RT-positive control with RNA from an IgG-expressing cell line with enzyme; lane 9 shows an RT-negative control in which enzyme was omitted from the RT reaction. Molecular size standards in bp are shown on the right.

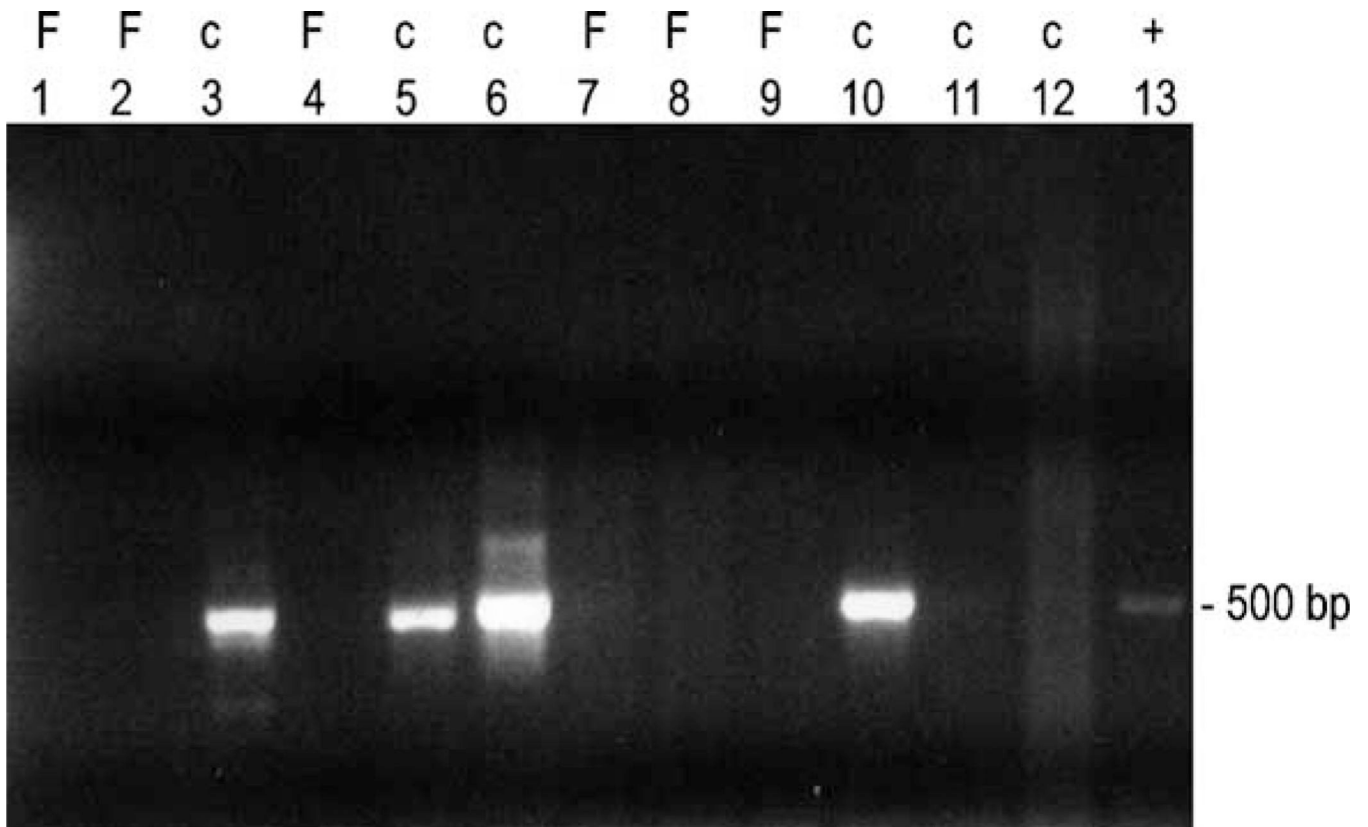


Fig. 3. Nested PCR comparing the freeze–thaw method to performing RT on the cap surface. PCR was performed on reverse-transcribed cDNA after freeze–thawing one cell per cap (lanes 1, 2, 7, and 9) or three cells per cap (lanes 4 and 8), or after performing RT on cap surfaces containing one cell (lanes 3, 6, 10, 11) or three cells (lanes 5 and 12). Performance of RT on the cap surface yielded PCR products in four of six caps, including three caps containing single CD38⁺ cells (lanes 3, 5, 6, and 10). Freeze–thawing of cells yielded one faint product (lane 7). F indicates the freeze–thaw method; C indicates that RT was performed on the cap surface; “+” indicates control cDNA reverse-transcribed from the IgG-expressing cell line (lane 13). Approximate size of the amplification product in bp is indicated on the right.

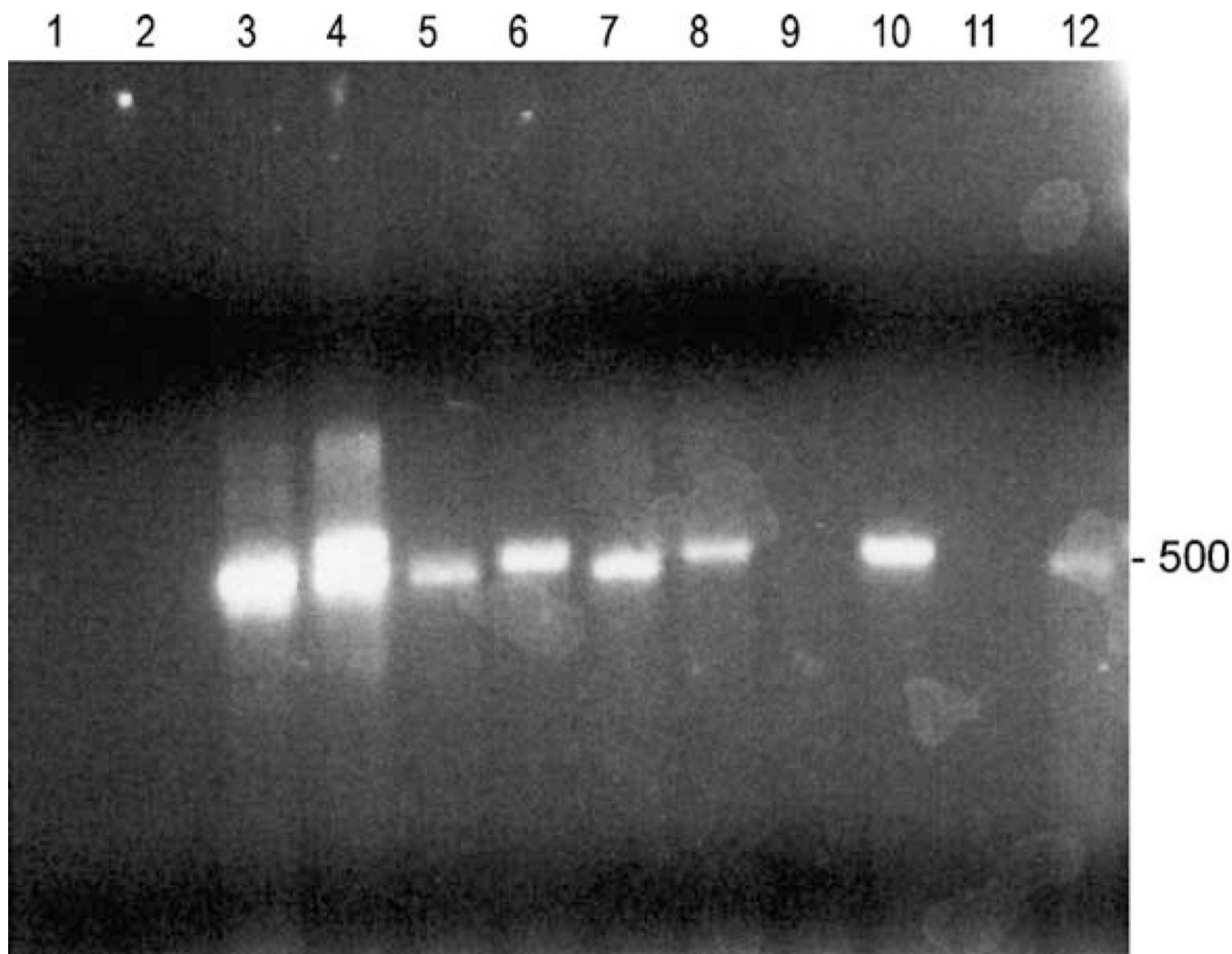


Fig. 4. Nested PCR of additional RT after overnight freeze–thaw of caps. Twelve caps from Fig. 3 were frozen overnight at -80°C , and RT was repeated on all cap surfaces. Eight of the twelve caps yielded PCR products, including the five that were previously observed (lanes 3, 5, 6, 7, and 10). RT on the caps also revealed additional products in three of five previously negative caps (lanes 4, 8, and 12). Approximate size of the amplification product in bp is indicated on the right.

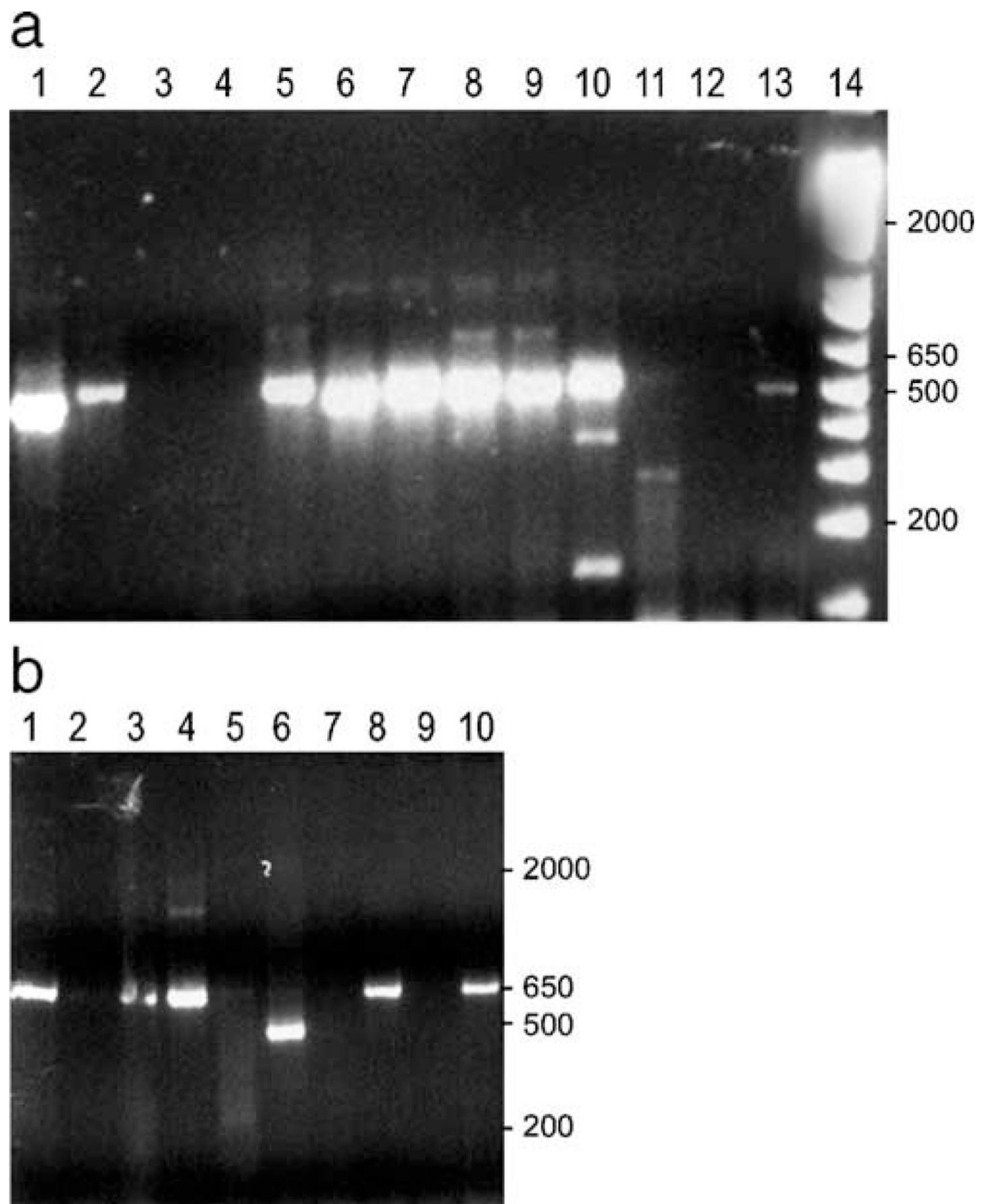


Fig. 5. Nested PCR of individual LCM-captured cells. (a) RT was performed on cap surfaces containing single CD38⁺ cells, followed by PCR amplification using IgG heavy chain primers. Ten of the 13 caps yielded heavy chain products (lanes 1, 2, 5–11 and 13). Molecular size markers in bp are indicated on the right (lane 14). (b) cDNA from the ten caps that amplified heavy chain sequences were further subjected to nested PCR amplification of kappa light chains, resulting in the identification of seven kappa light chain products (lanes 1, 3, 4–6, 8 and 10). Molecular size markers in bp are indicated on the right.